Electrical properties and shape-memory behavior of self-assembled carbon nanofiber nanopaper incorporated with shape-memory polymer

2010 Smart Mater. Struct. 19 075021

(http://iopscience.iop.org/0964-1726/19/7/075021)

Smart Mater. Struct. **19** (2010) 075021 (7pp) doi:10.1088/0964-1726/19/7/075021

Electrical properties and shape-memory behavior of self-assembled carbon nanofiber nanopaper incorporated with shape-memory polymer

Haibao Lu[1,2], **Yanju Liu**[1], **Jihua Gou**[2,3], **Jinsong Leng**[1,3] **and Shanyi Du**[1]

[1] Center for Composite Materials and Structures, Harbin Institute of Technology, Harbin 150001, People's Republic of China
[2] Composite Materials and Structures Laboratory, Department of Mechanical, Materials and Aerospace Engineering, University of Central Florida, Orlando, FL 32816, USA

E-mail: jgou@mail.ucf.edu and lengjs@hit.edu.cn

Received 27 April 2010, in final form 17 May 2010
Published 16 June 2010
Online at stacks.iop.org/SMS/19/075021

Abstract
The present paper studies the electrical and shape-memory behavior of self-assembled carbon nanofiber (CNF) nanopaper incorporated with shape-memory polymer (SMP). The morphology and structure of the self-assembled nanopapers were characterized with scanning electron microscopy (SEM). A continuous and compact network was observed from the SEM images, which indicates that the CNF nanopaper could have highly conductive properties. The electrical conductivity of the CNF nanopaper was measured by the four-point probe method and its temperature coefficient effect was studied. Finally, the actuation of SMP was demonstrated by the electrical resistive heating of the CNF nanopaper.

(Some figures in this article are in colour only in the electronic version)

1. Introduction

Since the discovery of carbon nanotubes (CNTs) in 1991 [1], numerous studies have been reported on the remarkable physical and mechanical properties of CNTs and CNFs. The elastic modulus of carbon material is approximately comparable to that of diamond (1.2 TPa). The reported tensile strength of CNFs (5 GPa) is higher than that of high-strength steel (2 GPa) [2]. The electrical current-carrying capability of CNFs was estimated to be 1×10^9 A cm^{-2}. The copper wire was burned out at 1×10^6 A cm^{-2} [3]. The thermal conductivity of CNFs was predicted to be approximately 12 W m^{-1} K^{-1} [4]. The thermal conductivity of insulating polymer materials ranges from 0.15 to 0.30 W m^{-1} K^{-1}. Potential applications of CNTs and CNFs include nano-biotechnology [5], nano-systems [6], nanoelectronics [7], and nano-structured materials [8]. They have proven to be excellent additives to impart polymers with electrical conductivity at a relative lower loading. They are ideal nano-fillers to transform electrically non-conducting polymers into conductive materials. Therefore, they are highly sought-after candidate materials to replace traditional conductive fillers for insulating polymers. Although a variety of methods have been used to incorporate CNFs into polymers, the resulting composite could not achieve a high electrical conductivity to meet the practical requirements. A higher loading level is required to achieve a high conductivity of the composite. Unfortunately, this process could introduce some processing challenges. Due to strong attractive interactions, nano-fillers tend to aggregate to form agglomerates when dispersed into polymers, thus preventing an efficient transfer of the properties of nano-fillers to the polymer matrix. In addition, a high surface area of nano-sized particles results in a high viscosity of the matrix, which makes it difficult to achieve a uniform dispersion. Both obstacles could seriously block the connections between conductive fillers [9]. The increase in electrical conductivity of the composite is therefore limited due to the lack of effective connections.

[3] Authors to whom any correspondence should be addressed.

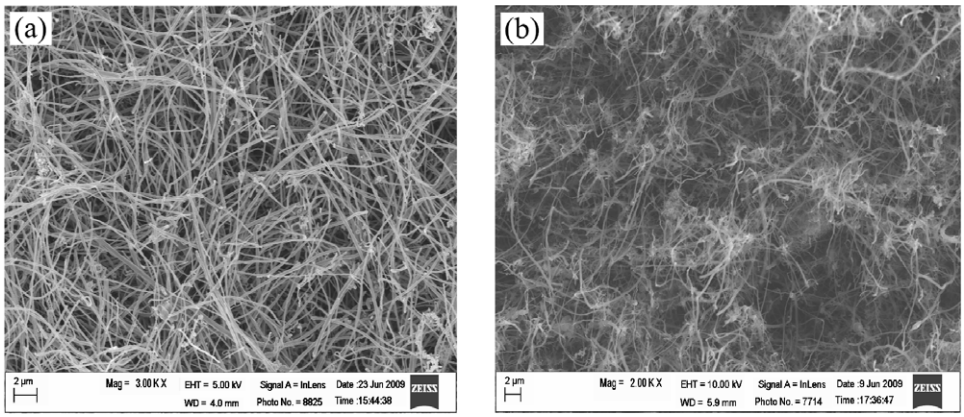

Figure 1. Morphologies and network structure of carbon nanofiber in nanopaper structures at a size of 2 μm observed from (a) a surface-section and (b) a cross-section, respectively.

A unique concept of making nanocomposites from CNF or CNT nanopaper has been explored [10]. Self-assembled arrays of CNFs or CNTs is particularly important to enable fundamental studies and applications [11, 12]. These attempts have been inspired by the successful manufacturing of single-walled carbon nanotube buckypaper. Potential applications of the CNF nanopaper are very promising, including fire protection [13], lightning strike protection (with an unusually high current-carrying capability) [14], electromagnetic interference shielding, and nanopaper-based composites. In this study, the CNF nanopaper was fabricated through the infiltration of the suspension of well-dispersed CNFs. The electrical resistivity of the nanopaper was determined by the four-point probe method. The dependence of electrical resistivity of the nanopaper on the thickness and ambient temperature was examined. The function of CNF nanopaper in SMP actuation was achieved by electrical resistive heating.

2. Experimental details

CNFs (Pyrograf®-III, PR-HHT-25) were supplied from Applied Sciences Inc., Cedarville, Ohio, USA. They were further heat treated at a temperature of 2200 °C, to obtain a complete graphitic structure and purified to a very high level (>99 wt%). Such heat treatment could also help to reduce the iron catalyst content to a very low level (<0.8 wt%). The nanofibers have a diameter of 50–100 nm and length of 30–100 μm. The CNFs were dispersed into distilled water with a non-ionic surfactant $C_{14}H_{22}O(C_2H_4O)_n$ (Triton X-100, supplied from BYK-Chemie USA, Inc, Wallingford, Connecticut, USA). A hydrophilic polycarbonate membrane (HTTP Isopore™ membrane filter) with a diameter of 142 mm was supplied from Millipore Co., Billerica, MA. The styrene-based SMP (Veriflex®S, VF 62) was purchased from Cornerstone Research Group (CRG) Inc., Dayton, Ohio. The Veriflex®S resin is a two-part, fully formable thermosetting resin system. The resin is engineered with a glass transition temperature (T_g) of 62 °C. The styrene resin was polymerized with the dibenzoyl peroxide hardener at a weight ratio of 24:1. The cured SMP with a density of 0.92 g cm^{-3} can change from a rigid glassy state to an elastic state when heated above a certain temperature.

3. Fabrication, electrical properties and function of CNF nanopaper

3.1. Fabrication of CNF nanopaper

The as-prepared CNFs of 0.6 g were mixed into 600 ml distilled water to form a CNF suspension. The non-ionic surfactant $C_{14}H_{22}O(C_2H_4O)_n$ (or sodium lauryl sulfate) of 2 ml was added to aid the dispersion of CNFs. The suspension was sonicated with a high-intensity sonicator (MISONIX Sonicator 4000, Qsonica, LLC, Newtown, Connecticut, USA) at room temperature for 15 min. After the initial sonication, both CNF suspension and probe were cooled down to room temperature. The sonication was performed again for another 15 min under the same condition. The CNF suspension was then filtrated through a 0.4 μm hydrophilic polycarbonate membrane under a high pressure to form a CNF nanopaper. After the filtration, the CNF nanopaper was further dried in an oven at 120 °C for 2 h to remove the remaining water and surfactant.

3.2. Morphology and structure of CNF nanopaper

SEM (ZIESS Ultra-55) was used to study the structure of the CNF nanopaper. Figures 1(a) and (b) are the typical surface and side views of the raw CNF arrays, respectively. The nanopaper has a porous structure with CNFs entangled with each other. The CNFs have a diameter ranging from 50 to 100 nm. No large aggregates were found, indicating a uniform distribution and close packing of CNFs in the nanopaper. A network structure was formed by the molecular interaction and mechanical interlocking between individual nanofibers, as shown in figure 1(a). Such a continuous network made of individual CNFs acts as conductive path for electrons, making the nanopaper electrically conductive. The network structure depends on the quality of the dispersion of the nanofibers. Figure 1(b) shows a uniform dispersion of CNFs under the above processing conditions.

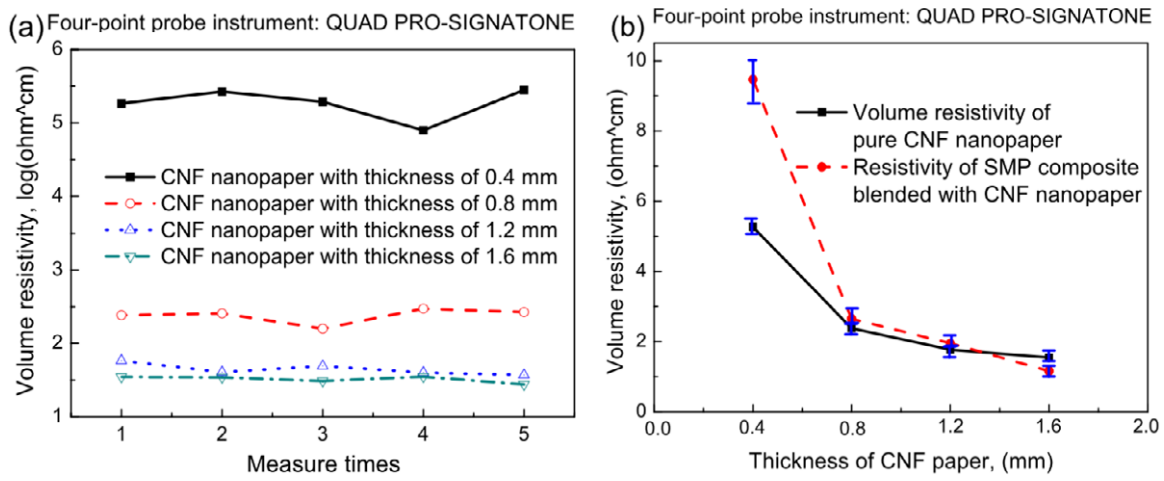

Figure 2. (a) Electrical resistivity of pure CNF nanopapers (each is measured five times), (b) electrical resistivity curves of pure CNF nanopaper and the SMP composite.

3.3. Electrical resistivity measurement

The electrical resistivities of the nanopaper and its enabled nanocomposite were measured with a SIGNATONE QUADPRO system, incorporated with a four-point cylindrical probe. The apparatus has four probes in a straight line with an equal inter-probe spacing of 1.56 mm. The radius of the probe needle is 100 μm. A constant current passes through the two outer probes and an output voltage is measured across the inner probes with a voltmeter. The electrical resistivity is given by

$$R_s = 4.53 \times \frac{V}{I} \tag{1}$$

where R_s is the electrical resistance, V is the voltage applied on the two inner probes, and I is the electrical current passing through the two outer probes.

The electrical resistivity of the test sample is therefore obtained as

$$\rho = R \cdot \frac{wt}{l} \tag{2}$$

where ρ is the electrical resistivity, R is the electrical resistance, and l, w, t are the length, width, and thickness of the sample. The electrical resistance was measured with a DC power supply.

The electrical resistivities of the nanopapers with different thicknesses are plotted against different locations, as shown in figure 2(a). Each data point denotes the resistivity at a particular zone. The error bar represents a standard deviation to show the variability in electrical resistivity of the test samples. As the thickness of CNF nanopaper increased from 0.4 to 1.6 mm, the average electrical resistivity of the nanopaper decreased from 5.268 to 1.544 Ω cm. The more CNFs in the nanopaper, the more conductive paths are formed in the CNF network. Given more conductive paths, more electrons are involved in an electrical circuit. Therefore, the amplitude of electrical current and current-carrying capability increase. In addition, more conductive paths will increase the probability of forming relatively shorter distances for a reduced electrical resistance to the electrical current. These mechanisms would significantly improve the electrical conductivity of the nanopaper.

As shown in figure 2(b), the change in electrical resistivity of the CNF nanopapers and their composites was studied as a function of thickness of the nanofibers. All the thickness of the four composite samples with various weight concentration of CNF nanopaper is 6 mm, where the thicknesses of the nanopapers with 0.6, 1.2, 1.8, 2.4 g nanofibers are 0.4, 0.8, 1.2 and 1.6 mm, respectively. Therefore the weight ratios of nanopapers in the composite are approximately 1.47%, 3.10%, 4.95% and 7.02%, respectively. From these two curves, the resistivity of the composite with a relatively smaller thickness of nanofibers is higher than the corresponding nanopaper. While the resistivity of the composite with a relatively larger thickness of nanofibers is lower than the corresponding nanopaper. The interaction between the polymer and nanopaper could contribute to it. The nanopaper has a porous structure. In the fabrication of the composite, the polymer resin will penetrate into or even through the nanopaper, occupying the pores in the nanopaper. When the pores are filled with the polymer, the density of the nanopaper will be changed because the bonding between CNFs is changed from the van der Waals force to the chemical linking provided by the polymer. Therefore, the electrical resistivity of the nanopaper will be altered, as a result of the distribution of CNFs re-arranged in the nanopaper. The electrical conductive path and network are reset, making the electrical properties of the nanopaper different.

When the nanopaper contains a relatively low weight concentration of CNFs, the volume fraction of the pores in the nanopaper is high. When the pores are filled by the insulating polymer, the conductive network could be destroyed or obstructed. Therefore, the electrical resistivity of the composite becomes higher than the corresponding nanopaper. While the nanopaper has a high weight concentration of CNFs, the volume fraction of the pores in the nanopaper becomes low. Therefore, the polymer could not destroy or obstruct the conductive network. On the other hand, the polymer could make the conductive network structure of the nanopaper more

compact due to the chemical bonding provided by the polymer and polymer matrix. Therefore, the electrical resistivity of the composite is lower than its corresponding pure nanopaper. However, this change is very slight because this interaction only occurs in a small domain. These changes can be seen from the experimental results plotted in figure 2(b).

3.4. Temperature-dependent electrical resistivity

The temperature range for the application of the nanopaper and its composite is generally from room temperature to 100 °C. Therefore, the temperature dependency of the electrical resistivity in this temperature range should be considered. The dependence was studied by measuring the electrical resistance while heating the specimen to a certain temperature.

The temperature coefficient is the relative change of a physical property when the temperature is changed by 1 K. In the following formula, let $R(T)$ be the physical property and T be the absolute temperature at which the property is measured. T_0 is the reference temperature, ΔT is the difference between T and T_0, and α is the temperature coefficient. Based on these definitions, the physical property is given by

$$R(T) = R(T_0)(1 + \alpha \Delta T) \tag{3}$$

where α has a dimension of an inverse temperature (K^{-1}).

Positive temperature coefficient (PTC) and negative temperature coefficient (NTC) effects in conductive materials have been studied since the initial observation of this phenomenon [15]. A PTC effect implies that the conductivity of a material rises with the temperature, typically in a defined temperature range. On the other hand, a NTC effect implies that the conductivity of a material drops with the temperature. The NTC effect is characterized by the restoration of electrical conductivity upon heating the specimen. It is related to the mobility of electrons with a temperature increase [16]. In this study, the thermal effect of the CNF nanopaper was determined from the temperature-dependent electrical resistivity experiment. Nanopapers with different thicknesses of 0.4, 0.8, 1.2 and 1.6 mm were studied. Figure 3 shows the change in electrical resistivity of the four nanopaper samples with temperature from room temperature to 120 °C. All four nanopapers show a NTC effect, where the electrical resistivity decreased with the environmental temperature. For example, the initial and final values of electrical resistivity for 2.4 g CNF nanopaper are 1.544 Ω cm at room temperature and 0.906 Ω cm at 120 °C, respectively. The most important factor for the negative temperature dependence of conducting material was clearly demonstrated to be an increased charge transfer associated with the prolonged electric current [17]. As is well known, the nanofibers have been constructed with length-to-diameter ratios of up to 300–1000. The electrical behavior of CNFs is regarded as that of thin metallic wires, being generally explained on the basis of the Dingle theory [18]. This theory assumes the existence of a relaxation time and a spherical Fermi surface, similar to the Fuchs–Sondheimer theory of thin metallic films. Both these theories tackle the surface scattering through the Boltzmann transport equation, subject to the respective boundary conditions. It has been observed that the temperature coefficient of resistivity for individual wires is lower than the bulk values. This behavior will become significant for lower values of reduced diameter k (the ratio of wire diameter to the bulk mean free path) [19]. Both the wire and the bulk have been demonstrated to produce the NTC effect. With more CNFs being involved into the conductive nanopaper, the free paths in the nanopaper bulk therefore increase, resulting in the ratio of wire diameter to the bulk mean free path being reduced (as the diameter of CNFs is constant). These features impact the CNF nanopaper with a NTC behavior.

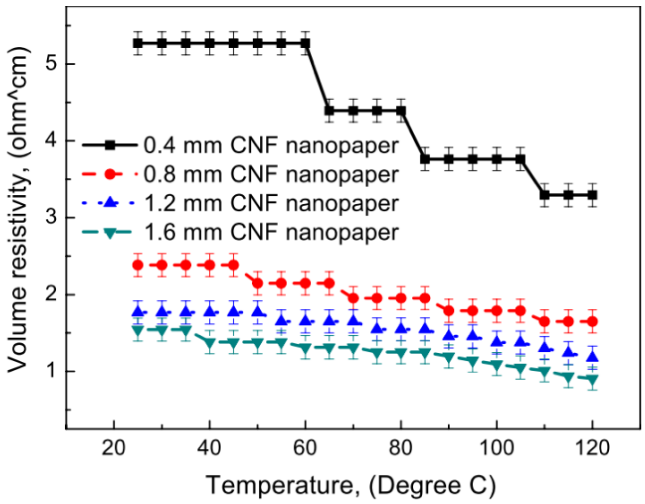

Figure 3. Temperature-dependent electrical resistivity of CNF nanopaper.

It was found that the nanopaper with 0.6 g CNFs showed an obvious change with the temperature. The electrical resistivity of the nanopaper decreased from 5.268 to 3.293 Ω cm as the temperature increased from room temperature to 120 °C. However, the electrical resistivity of the nanopaper with 2.4 g CNFs decreased from 1.544 to 0.906 Ω cm. CNF being a thermally steady material, the thermal expansion coefficient of an individual CNF is little affected by an increase in temperature, whereas the thermal expansion coefficient of the nanopaper bulk becomes significant, due to the nanopaper being composed of CNFs and air. The thermal expansion mismatch between individual nanofibers and the nanopaper bulk introduces an additional resistivity contribution, which becomes more and more sensitive to k as the k value is reduced [17]. Based on the SEM observation, the size and concentration of air in the nanopaper with a high weight of CNFs is smaller than that of the nanopaper with a low weight of CNFs. The thermal expansion mismatch between individual nanofibers and the latter nanopaper bulk becomes large. This increasing mismatch results in the mean conductive path length and electric current being prolonged. The above explanations and results assume significance in light of the fact that the prolonged electric current is associated with an increase in charge transfer. Therefore, the nanopaper with a lower weight concentration of CNFs (where in contrast, the weight concentration of air is high) exhibits a more obvious NTC effect.

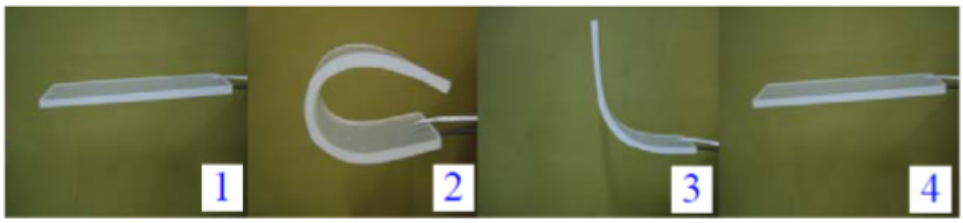

Figure 4. Series of photographs showing the macroscopic shape-memory effect of the pure SMP matrix. (Reprinted with permission from [16]. ©2010 Society of Chemical Industry.)

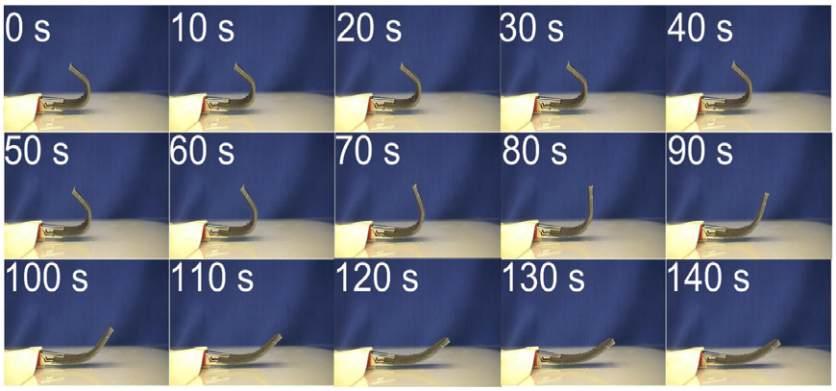

Figure 5. Series of photographs showing the macroscopic shape-memory effect of SMP composite integrated with 1.8 g CNF nanopaper. The permanent shape is a flat strip of composite material, and the temporary shape is deformed as a right-angled shape.

3.5. Function of CNF nanopaper in shape-memory polymer actuation

The polymer matrix used in the current study is a thermoset styrene-based SMP matrix consisting of two parts: the SMP resin and a curing agent. When curing, the resin and curing agent are mixed at a weight ratio of 24:1. The SMP resin was mixed with curing agent using a high shear mixer at a constant 600 rad min^{-1}. The resulting mixture was degasified in a vacuum oven to completely remove air bubbles. Nanopapers containing CNFs of 0.6, 1.2, 1.8 or 2.4 g were respectively attached on the bottom of the mold. The resin transfer molding process was used to make the SMP composite. The SMP resin was then injected into the mold. After mold filling, the mixture was cured in an oven with a ramp of approximately 1 °C min^{-1} from room temperature to 75 °C. The sample was then held at 75 °C for 3 h before being ramped to 90 °C at 15 °C/180 min. Finally, it was ramped to 110 °C at 20 °C/120 min. The thicknesses of the four composite samples with various weight concentrations of CNF nanopaper were all 6 mm, and the weight ratios of the nanopapers in the composite were approximately 1.47%, 3.10%, 4.95% and 7.02%, respectively.

Conductive CNF, CNT and graphite are nano-fillers that transform electrically non-conducting polymers into conductive materials. Extensive research has been done on conductive SMP composites by blending a small amount of conductive fillers [20–27]. However, the resulting composites still could not achieve a high enough electrical conductivity to meet the requirements [28–30]. A high loading level of filler is required to be blended into the SMP resin. A high viscosity of the SMP resin will result due to strong interactions between the resin and conductive filler, thus prevent an efficient transfer of the properties of the filler to the matrix and also make it difficult to have a uniform dispersion.

The shape-memory effect of the SMP matrix was presented in figure 4 [16]. One sample was shown as an example of a thermally induced shape-memory effect. The sample had an original flat shape, as shown in the first image. When the sample was heated above its switch transition temperature, it could be deformed to a desirable shape upon an external force. Cooling back below its switch transition temperature, a temporary shape was subsequently fixed, as shown in the second image. The sample was re-heated above its switch transition temperature, it started to recover from the temporary shape to its original shape. Being cooled down below its switch transition temperature, a second temporary shape is fixed, as shown in the third image. Finally, it could return to its original shape after the sample was heated again, as shown in the fourth image. From the thermally induced shape-memory process, it was found that the shape recovery behavior is inconvenient, uncontrollable, and discontinuous. A special heating source needs to be prepared and the energy loss is large. To overcome these limitations, a new actuation approach was used for the shape-memory effect by electrical resistive heating.

In this study, all the SMP composites were coated with one layer of the nanopaper containing different weight concentrations of CNFs through the resin transfer molding process. The function and effectiveness of the nanopaper in the actuation of SMP composites by electrical resistive heating were experimentally demonstrated. Figure 5 shows

the recovery of the SMP composite blended with 1.8 g CNF nanopaper as an electric current of 0.09 amplitude was applied. The shape recovery process of the flat (permanent shape) composite specimen with a dimension of $120 \times 20 \times 6$ mm was demonstrated. The thickness of CNF nanopaper is 1.2 mm.

The flat SMP specimen was bent as a 'U'-like shape (temporary shape) at 100 °C, and this temporary shape was kept until the specimen was cooled back to room temperature. No apparent recovery was found after the deformed sheet being kept in air for 2 h. A constant 8.4 V direct current voltage was applied to actuate the SMP composites. The shape recovery of the SMP composite was recorded by a video camera. It can be seen that the specimen took 140 s to complete the shape recovery. Initially the sample showed little recovery ratio during the first 20 s. It then started to exhibit a faster shape recovery behavior until 120 s. During the last 20 s, little change in the shape recovery was observed. The composite specimen did not show a 100% recovery ratio as it did not completely return to its initially flat shape. This small absence of complete shape recovery ratio could attribute to the interface friction between the nanopaper and the underlying SMP. The SMP part may lack enough mechanical strength to pull the nanopaper back to its original shape.

3.6. Electro-induced shape-memory recovery behavior

For practical application, shape recovery performance of SMP materials is extremely important. Therefore, a systematic shape recovery test of SMP specimens upon bending was performed. The procedure includes the following steps: (1) the specimen with its original rectangular shape is kept in a water bath for 5 min above its switching temperature; (2) the SMP specimen is bent to a storage angle θ_0 around a mandrel with a special radius, and then the specimen is kept in cool water with the external constraint to 'freeze' the elastic deformation energy for 5 min (storage); (3) the specimen fixed on the apparatus is resistively heated by applying an electrical current, and then it recovers to an angle θ_N (recovery). θ_0 is the original storage angle of the specimen in the storage state during the first bending cycle. θ_N is the residual angle in the recovery state during the N_{th} thermomechanical bending cycle ($N = 1, 2, 3, \ldots$).

$$R_r = \frac{\theta_0 - \theta_N}{\theta_0} \times 100\%, \qquad (0^\circ \leqslant \theta \leqslant 180^\circ). \qquad (4)$$

The electro-induced shape-memory effect of SMP composites was evaluated from the recovery angle with respect to shape recovery time. The recovery angle refers to the degree of SMP material in response to external stimuli in the shape recovery process. It was determined by measuring the angle between the two sides of the bent specimen. The flat composite specimens (permanent shape) with dimensions of 120 × 20 × 6 mm were bent to an 'n'-like shape (temporary shape) at 75 °C and remained this shape during cooling back to room temperature. The total bend angle of this deformation is 180°. The actuation of the SMP composite was carried out by an electrical current under a constant electric power of 0.8 W. It is found that a high

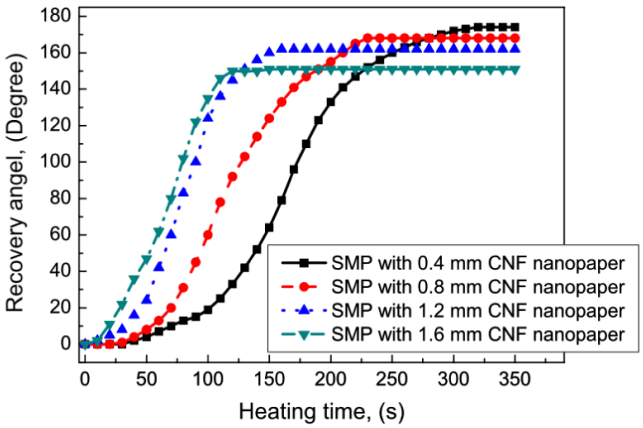

Figure 6. Electro-induced shape-memory behavior of SMP composites with various CNF nanopaper weight concentrations.

electrical resistive energy will result in a large quantity of heat and further make the interface bonding between polymer and nanopaper burn up. The reason that could account for this phenomenon is the tremendous difference in thermal conductivity of insulating SMP and conductive CNF nanopapers. The polystyrene SMP features an intrinsically low thermal conductivity 0.17 W m^{-1} K^{-1}. In comparison, the as grown CNF aggregate has a thermal conductivity of 12 W m^{-1} K^{-1}, while the heat treated individual CNF has an approximate thermal conductivity of 2000 W m^{-1} K^{-1}.

With a constant 0.8 W electric power, all four composite samples show electrically responsive behavior. As shown in figure 6, the SMP composite specimen blended with 2.4 g CNF nanopaper has the fastest response to the electrically resistive Joule heating (it completed shape recovery within 100 s). However, it has the lowest shape recovery ratio, approximately to 75%. Meanwhile, the SMP composite specimen layered with 0.6 g CNF nanopaper has the slowest response to the resistive Joule heating (it returned to the permanent shape within 320 s), but the shape recovery ratio was approximately to 95%. Therefore, the weight concentration of CNF nanopaper layered on the surface of SMP had a positive effect on the shape recovery speed but a negative effect on the shape recovery ratio.

A chemically cross-linked structure was formed by macromolecular chains during the curing process of the thermosetting SMP resin. The relative motion of macromolecule segments or domains is the primary mechanism of the shape-memory effect in the thermally responsive SMP materials. During the process of shape recovery, the packed macromolecule segments needed to overcome external constraints to regain their permanent shape. CNF nanopaper does not have a shape-memory effect and cannot return to the original configuration. It needs a recovery force provided by the SMP part to regain the original configuration. The opposing motion between the nanopaper and its underlying SMP yields an interfacial friction, which would prevent the shape deformation and recovery behavior of the SMP composite. However, the SMP macromolecule segments have a low recovery force to overcome the friction. Therefore, the

SMP composite could have a low shape recovery ratio with an increase in weight fraction of CNF nanopaper. However, the CNF nanopaper could significantly improve the electrical conductivity of the SMP composite to facilitate electrically resistive heating transfer from the nanopaper to the underlying SMP composite. Therefore, the speed of electro-active response was significantly improved with an increase in the CNF nanopaper content of the SMP composite.

4. Conclusions

A series of experiments were conducted to study the electrical and shape-memory behavior of the CNF nanopaper incorporated with SMP. The function in the SMP actuation was achieved by the electrical resistive heating of the CNF nanopaper. The temperature-dependent electrical resistivity of the CNF nanopaper showed an NTC effect. It could impart the CNF nanopaper with an NTC sensing capability in a certain temperature range. In addition, the actuation of SMP composites coated with 1.8 g CNF nanopaper was demonstrated by electrical resistive heating. The CNF nanopaper significantly improved the electrical conductivity to make the SMP composite have a fast response to an electrical resistive heating. However, the shape recovery ratio was reduced due to an interfacial friction between the nanopaper and underlying SMP.

Acknowledgments

The materials presented here are based upon work supported by National Science Foundation under grant no. CCMI-0757302. This work was also partially supported by Florida Center for Advanced Aero-Propulsion (FCAAP) Program under grant no. FSU#218007-530-024809-R010689. Any opinions, findings, and conclusions or recommendations expressed in this material are those of the authors and do not necessarily reflect the views of National Science Foundation.

References

[1] Iijima S 1991 Helical microtubules of graphitic carbon *Nature* **354** 56–8
[2] Manoharan M P, Sharma A, Desai A V, Haque M A, Bakis C E and Wang K W 2009 The interfacial strength of carbon nanofiber epoxy composite using single fiber pullout experiments *Nanotechnology* **20** 295701
[3] Li C, Thostenson E T and Chou T W 2008 Effect of nanotube waviness on the electrical conductivity of carbon nanotube-based composites *Compos. Sci. Technol.* **68** 1445–52
[4] Yu C 2006 Thermal contact resistance and thermal conductivity of a carbon nanofiber *J. Heat. Transfer.* **128** 234–9
[5] Williams K A, Veenhuizen P T M, Torre B G, Eritja R and Dekker C 2002 Nanotechnology: carbon nanotubes with DNA recognition *Nature* **420** 761–7
[6] Shirinyan A S and Wautelet M 2004 Phase separation in nanoparticles *Nanotechnology* **15** 1720–31
[7] Choi W B 2004 Aligned carbon nanotubes for nanoelectrics *Nanotechnology* **15** S512–6
[8] Prunele E 2005 Time evolution of wavepackets on nanostructures *J. Phys. A: Math. Gen.* **38** 4843–58
[9] Gou J, Braint S O, Gu H and Song G 2006 Damping augmentation of composites using carbon nanofiber paper *J. Nanomater.* **1** 1–7
[10] Gou J 2006 Single-walled nanotube buckypaper and composites *Polym. Int.* **55** 1283–8
[11] Koratkar N A, Wei B and Ajayan P M 2002 Carbon nanotube films for damping applications *Adv. Mater.* **14** 997–1000
[12] Koratkar N A, Wei B and Ajayan P M 2003 Multifunctional structural reinforcement featuring carbon nanotube films *Compos. Sci. Technol.* **63** 1525–31
[13] Zhao Z and Gou J 2009 Improved fire retardancy of thermoset composite modified with carbon nanofibers *Sci. Technol. Adv. Mater.* **10** 015005
[14] Gou J, Blanco R, Olmi C and Song G 2007 Synthesis and processing of carbon nanopaper for lightning strike protection of polymer composite structure *China: World Scientific* **1** 10–3
[15] He X J, Du J H, Ying Z, Cheng H M and He X J 2005 Positive temperature coefficient effect in multiwalled carbon nanotube/high-density polyethylene composites *Appl. Phys. Lett.* **86** 062112
[16] Lu H B, Yu K, Sun S H, Liu Y J and Leng J S 2010 Mechanical and shape-memory behavior of shape-memory polymer composites with hybrid fillers *Polym. Int.* **59** 766–71
[17] Sharma B K and Srivastava R 1983 Negative temperature coefficient of resistivity of thin metallic wires *J. Mater. Sci. Lett.* **2** 775–6
[18] Dingle R B 1970 The anomalous skin effect and the reflectivity of metal *Proc. R. Soc.* A **201** 545–56
[19] Larson D C 2001 Physics of thin films *Phys. Rev. Lett.* **468** 2364–7
[20] Leng J S, Lv H B, Liu Y J and Du S Y 2007 Electroactivate shape-memory polymer filled with nanocarbon particles and short carbon fibers *Appl. Phys. Lett.* **91** 144105
[21] Leng J S 2008 Electrical conductivity of shape memory polymer embedded with micro Ni chains *Appl. Phys. Lett.* **92** 014104
[22] Leng J S, Huang W M, Lan X, Liu Y J and Du S Y 2008 Significantly reduceing electrical resistivity by forming conductive Ni chains in a polyurethane shape-memory polymer/carbon-black composite *Appl. Phys. Lett.* **92** 204101
[23] Leng J S, Lv H B, Liu Y J and Du S Y 2008 Synergic effect of carbon black and short carbon fiber on shape memory actuation by electricity *J. Appl. Phys.* **104** 104917
[24] Buckley P R, McKinley G H, Wilson T S, Small W IV, Benett W J, Bearinger J P, McElfresh M W and Maitland D J 2006 Inductively heated shape memory polymer for the magnetic actuation *IEEE Trans. Biomed. Eng.* **53** 2075–83
[25] Mohr R, Kratz K, Weigel T, Lucka-Gabor M, Moneke M and Lendlein A 2006 Initiation of shape-memory effect by inductive heating of magnetic nanoparticles in thermoplastic polymer *Proc. Natl Acad. Sci. USA* **103** 3540–6
[26] Lu H B, Liu Y J, Gou J, Leng J S and Du S Y 2010 Synergistic effect of carbon nanofiber and carbon nanopaper on shape memory polymer composite *Appl. Phys. Lett.* **96** 084102
[27] Leng J S, Lan X, Liu Y J and Du S Y 2009 Electroactive shape-memory polymer composite filled with nano-carbon powders *Smart Mater. Struct.* **18** 074003
[28] Liu Y J, Lv H B, Lan X, Leng J S and Du S Y 2009 Review of electro-active shape-memory polymer composite *Compos. Sci. Technol.* **69** 2064–8
[29] Meng Q H and Hu J L 2009 A review of shape memory polymer composites and blends *Composites* A **40** 1661–72
[30] Leng J S, Lu H B, Liu Y J, Huang W M and Du S Y 2009 Shape-memory polymers-A class of novel smart materials *MRS Bull.* **34** 848–55